Shear in Structural Stability: On the Engesser–Haringx Discord

Johan Blaauwendraad
Professor Emeritus of Structural Mechanics
Delft University of Technology,
Private: Klinkenbergerweg 74,
6711 ML Ede, The Netherlands
e-mail: j.blaauwendraad@tudelft.nl

Since Haringx introduced his stability hypothesis for the buckling prediction of helical springs over 60 years ago, discussion is on whether or not the older hypothesis of Engesser should be replaced in structural engineering for stability studies of shear-weak members. The accuracy and applicability of both theories for structures has been subject of study in the past by others, but quantitative information about the accuracy for structural members is not provided. This is the main subject of this paper. The second goal is to explain the experimental evidence that the critical buckling load of a sandwich beam-column surpasses the shear buckling load GA_s, which is commonly not expected on basis of the Engesser hypothesis. The key difference between the two theories regards the relationship, which is adopted in the deformed state between the shear force in the beam and the compressive load. It is shown for a wide range of the ratio of shear and flexural rigidity to which extent the two theories agree and/or conflict with each other. The Haringx theory predicts critical buckling loads which are exceeding the value GA_s, which is not possible in the Engesser approach. That sandwich columns have critical buckling loads larger than GA_s does, however, not imply the preference of the Haringx hypothesis. This is illustrated by the introduction of the thought experiment of a compressed cable along the central axis of a beam-column in deriving governing differential equations and finding a solution for three different cases of increasing complexity: (i) a compressed member of either flexural or shear deformation, (ii) a compressed member of both flexural and shear deformations, and (iii) a compressed sandwich column. It appears that the Engesser hypothesis leads to a critical buckling load larger than GA_s for layered cross section shapes and predicts the sandwich behavior very satisfactory, whereas the Haringx hypothesis then seriously overestimates the critical buckling load. The fact that the latter hypothesis is perfectly confirmed for helical springs (and elastomeric bearings) has no meaning for shear-weak members in structural engineering. Then, the Haringx hypothesis should be avoided. It is strongly recommended to investigate the stability of the structural members on the basis of the Engesser hypothesis. [DOI: 10.1115/1.3197142]

Keywords: stability, Engesser theory, Haringx theory, shear-weak member, shear deformation, thick-faced sandwich, structural engineering

1 It Starts With Buckling of Helical Springs

On May 30, 1942, Professor C. B. Biezeno addressed the science section of the Royal Academy of Sciences in The Netherlands (KNAW) on an interesting stability subject. He reported "On the buckling and lateral rigidity of helical compression springs," a paper by J. A. Haringx [1], an employee—later on director—of the physics laboratory at Philips Co. in The Netherlands. After World War II this study received a place in his doctoral thesis supervised by Professor Biezeno, of which an English translation was published in 1947 [2]. Buckling of compressed helical springs was already studied earlier in 1924 by Grammel [3], in 1925 by Biezeno and Koch [4], and was also dealt with in the book of Biezeno and Grammel in 1939 [5]. What they all had in common is that they modeled the helical spring as a beam-column and accounted for the length l_0 of the unloaded spring, the mean spring diameter D, the compressional rigidity EA, and the flexural rigidity EI to describe the theory. These rigidities depend on the number of coils over the length l_0, the mean spring diameter, the wire diameter, the pitch, and the material properties (Young's modulus E and Poisson's ratio m, reciprocal value of the more often used ν). The slenderness ratio l_0/D is a common parameter in their theories, but important differences occur. Grammel only accounted for the compressional and flexural rigidity, whereas Biezeno and Koch additionally took into account the shear rigidity GA_s. It is interesting in the theory of Grammel that a bounding value $l_0/D \approx 3.3$ was obtained, such that buckling is nonexisting for lower values. This phenomenon did not occur in the (seemingly more accurate) theory of Biezeno and Koch. They predicted that buckling always can occur as long as the spring is not completely suppressed. However, tests performed by Haringx supported the findings of Grammel that indeed a lower bound for the slenderness ratio exists, be it that the tests showed a lower ultimate slenderness ratio $l_0/D \approx 2.7$. The remarkable thing is that the likely more sophisticated theory of Biezeno and Koch, additionally accounting for shear rigidity in the way proposed by Engesser in Ref. [6], failed to predict the phenomenon, whereas the less accurate theory of Grammel did, be it in a slightly unsafe way. Haringx' contribution was the development of a modified theory, which accounts for all three types of rigidity (flexure, shear, and compression), predicts a lower bound, and surprisingly well matches the test results. Biezeno was unmistakably pleased by these new results and considered them to be an advance on his own theory. From that time on the debate goes on whether we should follow Engesser or Haringx in structural stability studies.

2 Discussion of Literature Results

In the KNAW communication, Biezeno showed a figure of Haringx, here reproduced as Fig. 1. On the abcis the ratio l_0/D occurs, where l_0 is the length of the unloaded spring and D is the mean spring diameter. The quantity ξ on the ordinate is the ratio of the axial force and the compressional rigidity of the unloaded

Contributed by the Applied Mechanics Division of ASME for publication in the JOURNAL OF APPLIED MECHANICS. Manuscript received December 22, 2008; final manuscript received February 23, 2009; published online February 4, 2010. Review conducted by Robert M. McMeeking.

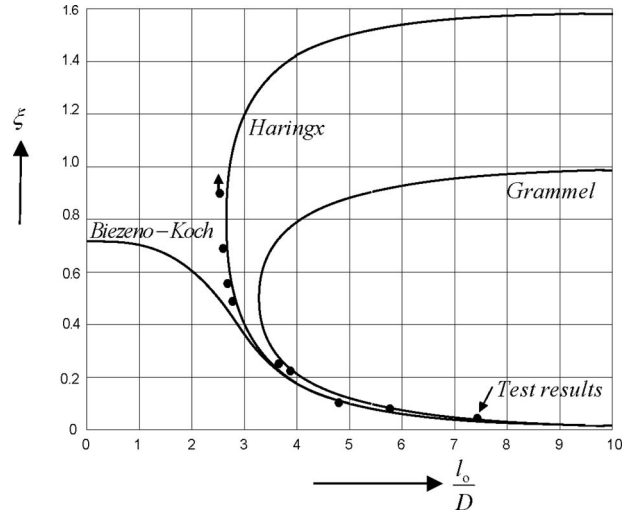

Fig. 1 Results of theories and tests for helical springs [1]

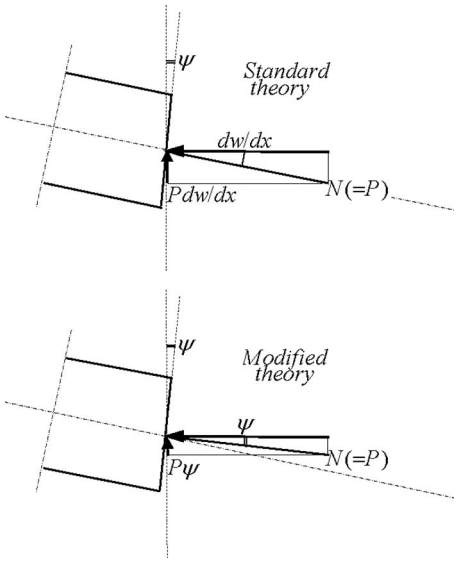

Fig. 2 Hypotheses of Engesser and Haringx on normal force direction, resulting in different ratio of shear force *V* and compressive load *P*

spring. Only the part of the graphs belonging to $\xi < 1$ has practical importance. The three graphs present the results of Grammel, Biezeno–Koch, and Haringx, respectively. "The isolated points represent experimental results obtained with springs of various lengths ($D=18$ mm, wire diameter of 0.5, 2 mm, pitch=5 mm); a vertical arrow indicates that the spring in question did not buckle if totally compressed" [1] and "most interesting is the behavior of a spring, the length of which is about 2.7 times its diameter. If the length exceeds this amount with some 5% the spring buckles under a compression of about 50%, whereas no stability at all occurs if the length is some 5% smaller [1]."

The most fundamental difference between the theory of Haringx and the two older ones of Grammel and Biezeno–Koch regards the assumption about the direction of the normal force N in the cross section, which has consequences for the relationship between the shear force V and the axial force P. Grammel and Biezeno–Koch started from a normal force *parallel to the beam axis* at the loaded state, a standard approach in mechanics reaching back to Engesser [6], and Haringx [1] choose the force N *normal to the cross section* at the state after loading, pitifully without stating expressly physical grounds or mechanic arguments for his deviating choice. These different hypotheses are visualized in Fig. 2.

For the combination of $l_0/D=2.7$ and $\xi=0.9$, the actual slenderness is $l/D=2.7(1-\xi)=0.27$, where l is the length of the spring after compression. The length of the spring is about a quarter of the spring diameter. Does it go without saying to still consider such a spring as a beam-column? Such a highly compressed spring is rather a stub and the end effects of such a member may have rather big influence.

It remains that the Haringx' graph matched his test results very well and therefore can be applied safely to the buckling of the helical springs. The important question remains on whether his theory is also reliable in structural engineering (framed structures). Before answering this, two more things must be said. First, a big difference between helical springs and structural beam-columns regards the compressibility. For springs the compression can become up to 50%, whereas shortening of compressed structural columns is justifiably neglected for structural members of isotropic and composed cross sections like sandwich columns. Second, it must be realized that Haringx could not verify his theory for the full range of possible combinations of flexural and shear rigidities. In helical springs their ratio is [5]

$$\frac{EI}{GA_s} = \frac{1}{8+4\nu} D^2 \tag{1}$$

which is determined by the mean spring diameter D and Poisson's ratio ν (value of 0.3 for steel) and cannot be varied at wish. Haringx has worked with a constant D and ν in all tests, hence the ratio of the critical flexural buckling force and critical shear buckling is in a rather small bandwidth. Therefore, he did not check the validity of his theory for pronounced cases of a structural shear-weak member or a shear-rigid one. Better said, it just was not relevant for him. Therefore, the reliability of the model of Haringx for structural members needs to be confirmed separately. A first attempt was made in 1982 by Ziegler [7], who was interested in the subject since the 1940s of the last century. He choose a more fundamental approach than Engesser did, in so far that he also accounted for the axial strain of the buckled bar. He arrived at two important conclusions. The theory of Engesser for a bar of both flexural and shear deformations is correct, when the flexural rigidity EI in his theory is replaced by $EI/(1-\varepsilon)$ and the shear rigidity GA_s by $GA_s/(1-\varepsilon)$, where ε is the axial shortening strain and GA_s is the effective area for shear deformation. For structural members it holds $\varepsilon \ll 1$; hence, this refinement is not worth considering. His second conclusion regards the question why Haringx did match his tests so well. The long and the short of his account is the consideration that the helical spring is essentially different from a beam-column with flexural, shear, and axial rigidities.

Ziegler's study is restricted to the question of which theory is most correct and did not achieve at conclusions on the degree of inaccuracy of Haringx' theory.

Timoshenko and Gere [8] discussed in their book the effect of shearing deformation on the critical buckling load. In fact they presented two approaches: one "standard" referring to Engesser's and one "modified," referring to Haringx'. The latter theory is discussed in the small print of the related book article, but is accompanied by the statement saying that "the modified method may be more accurate for cases in which the effect of shear is unusually large, although the standard method is more on the safe side."

Bažant and Beghini addressed the subject in the context of shear buckling of sandwich, fiber composite, and lattice columns [9–11]. Their theoretical studies arrive at a similar conclusion on

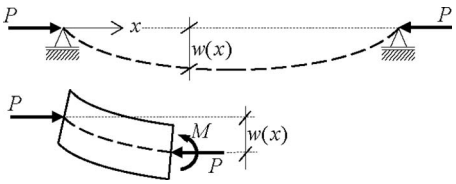

Fig. 3 Simply-supported member; force and moment in cross section

the validity of the theory of Haringx for structural members. They did not make a clear statement about the extent of the inaccuracy, either.

In recent studies of Attard and Hunt, the subject is at stake again. In Ref. [12] they discussed the buckling of a member of an isotropic cross section using a hyperelastic description of the constitutive law. Their study has special meaning for short columns, anticlastic transverse curvature, and large width to thickness ratio. Different from Ziegler and Bazant, they concluded that their findings confirm the Haringx hypothesis. In Ref. [13] they derived a new formula for the buckling of sandwich beam-columns, again on hyperelastic basis and consistent with the Haringx hypothesis, which fits their test results and of Fleck and Sridhar [14]. Here, again, they conclude in favor of Haringx. They showed their formula to be equivalent to Allen's formula for thick-faced sandwiches. The value GA_s is known as an upper limit in the Engesser theory for shear-weak beam-columns, whereas the Haringx theory is able to predict larger values. Tests for shear-weak sandwiches show that the value GA_s for the critical buckling load can be surpassed. The question can be raised if the Haringx hypothesis explains this observation.

In the present paper we discuss the results of Timoshenko and Gere because they nicely clarify the differences and after that we will derive the buckling formulas on the basis of a thought experiment, solving the problem from a viewpoint appealing to structural engineers. This will be done for a number of cases of increasing complexity. In the opinion of the present author the newly derived formulas show the primacy of the Engesser hypothesis in the structural engineering domain.

3 Investigation of the Timoshenko–Gere Solutions

The findings of Timoshenko and Gere [8] will be presented in the notation of the present paper. Consider the incompressible, simply-supported beam-column in Fig. 3 of length l, flexural rigidity EI, and shear rigidity GA_s. For reasons of convenience we introduce two buckling loads P_b and P_s for the beam-column.

$$P_b = \frac{\pi^2 EI}{l^2}, \quad P_s = GA_s \tag{2}$$

where P_b is the Euler buckling load for a beam-column in bending with flexural rigidity EI. Explanation of the physical meaning of the quantity P_s is postponed to hereafter. The derivations of Timoshenko and Gere can be interpreted to yield the following eigenvalue problems:

$$\text{Standard (Engesser)}: (PP_b + PP_s - P_bP_s)\hat{w} = 0 \tag{3}$$

$$\text{Modified (Haringx)}: (P^2 + PP_s - P_bP_s)\hat{w} = 0 \tag{4}$$

where $\hat{w}$ is the deflection at midspan. The only difference is in the first term inside the brackets: PP_b and P^2, respectively. Therefore, for a critical value P sufficiently close to P_b the differences between the methods of Engesser and Haringx vanish. This is the case for relatively large shear rigidity.

For shear-weak cases the difference is not immediately clear. At buckling it holds $\hat{w} \neq 0$; hence, the term between the brackets is zero. Engesser ends up with a linear equation in P and Haringx with a quadratic one. Their solutions are as follows:

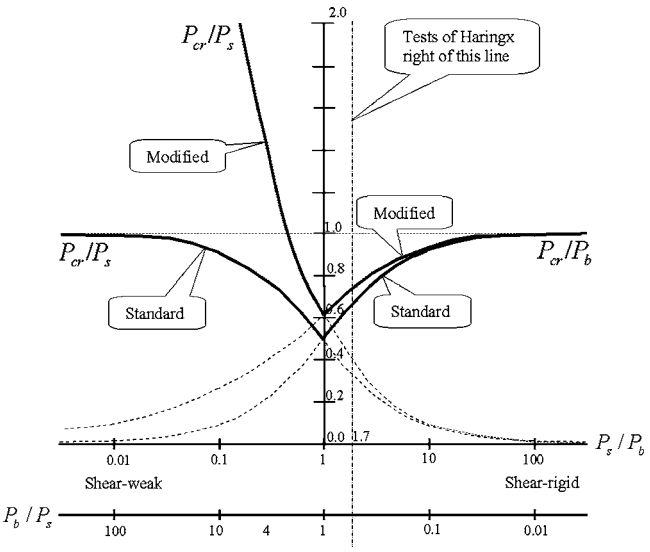

Fig. 4 Ratios P_{cr}/P_b and P_{cr}/P_s as function of P_s/P_b and P_b/P_s; plots for standard and modified theories

$$\text{Engesser}: P_{\text{cr}} = P_sP_b/(P_s + P_b) \tag{5}$$

$$\text{Haringx}: P_{\text{cr}} = \frac{1}{2}(-P_s + \sqrt{P_s^2 + 4P_sP_b}) \tag{6}$$

The Engesser solution meets the condition that $P_{\text{cr}} = P_b$ for very large shear rigidity. The extreme of a very large flexural rigidity yields $P_{\text{cr}} = P_s$. The buckling load P_{cr} can neither exceed P_b nor P_s. Therefore, GA_s is an upper limit in Engesser's theory for a beam-column with flexural and shear deformations. The Haringx solution also meets the condition that $P_{\text{cr}} = P_b$ for very large shear rigidity; however, an increasingly large $P_{\text{cr}} = \sqrt{P_bP_s}$ is obtained for increasing flexural rigidities, which is very different from the limit value P_s due to the Engesser hypothesis.

In Fig. 4 the prediction of the critical buckling load is shown for the full range of the ratio P_b/P_s. This is done for the result of the standard theory in Eq. (5) and for the outcome of the modified theory in Eq. (6). This is done twice: the first time is when the dimensionless critical load P_{cr}/P_b is plotted and the second time is when P_{cr}/P_s. The right-hand part of the figure holds for shear-rigid beam-columns ($P_s/P_b \gg 1$) and the left-hand part is for the shear-weak ones ($P_b/P_s \gg 1$). In the right-hand part one best looks at the value of P_{cr}/P_b and in the left-hand part to the values of P_{cr}/P_s. On the horizontal axis the ratios are plotted in a logarithmic scale. It is seen in the right-hand part of the figure that both the standard and modified theories correctly approach the upper limit $P_{\text{cr}}/P_b = 1$ for large values of P_s/P_b. For values of $P_s/P_b > 1$ the difference between the standard and the modified methods remains small (bold lines in the right-hand part). It is this part of the figure, which is shown by Timoshenko and Gere [8]. However, for the domain $P_s/P_b < 1$, the difference is increasing substantially (dotted curves in the left-hand part of the figure). The difference is even better demonstrated by the plot of P_{cr}/P_s as a function of P_b/P_s (bold lines in the left-hand part of the figure, dotted lines in the right-hand part). Now the limit $P_{\text{cr}}/P_s = 1$ is seriously surpassed.

The author of the present paper is of the opinion that the solution on the basis of the Haringx hypothesis cannot be true for structural engineering applications in building and civil engineering. To ground this we consider the example of a horizontal beam-column of large flexural rigidity EI and small shear rigidity GA_s. The reader could, for instance, take in mind a Vierendeel beam. The beam-column is simply-supported and loaded by compressive axial forces P at both ends (see Fig. 5). At buckling the flexural

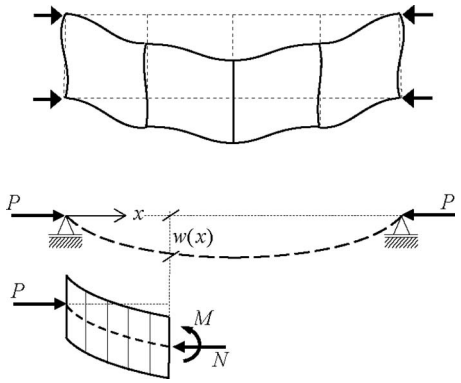

Fig. 5 Vierendeel girder; example of "member" in pure shear

deformation in this member is negligible, only shear deformation occurs. The critical buckling load of the Vierendeel beam can be studied by a finite element analysis (FEA). The result will be a finite effective shear rigidity GA_s. In the replacing beam-column representation all sections along the span are kept in a parallel position, and for reasons of symmetry this position is vertical. Hence, the shear deformation is $\gamma = dw/dx$, where w is the vertical displacement and the shear force is $V = GA_s dw/dx$. At buckling this shear force is nonzero. On the other hand the vertical position of all cross sections means that the rotation ψ is zero all along the span. In view of the Haringx hypothesis $V = P_s \psi$, a nonzero V and zero ψ at buckling would imply that the critical load P_s is infinitely large. This is in conflict with the physical reality and the FEA result. The model of Haringx yields an erroneous result for this structural problem.

A closer look at the tests of Haringx in Fig. 4 learns that they all fall in the shear-rigid right-hand part of the plot. It can be calculated on the basis of Eq. (1), the slenderness ratio l_0/D, and accompanying compression ratio ξ in the tests that Haringx only verified his theory for ratios P_s/P_b to be larger than 1.7. At those values one is in the domain, in which the difference between the standard and the modified theories is relatively small.

4 Engineer's Derivation of Buckling Formulas

In this section, we will derive in a consistent way the critical buckling loads for structural members of increasing complexity: (i) a beam-column with either just flexural deformation (Euler–Bernoulli beam) or just shear deformation, (ii) the case of a beam-column with both flexural and shear deformations (Timoshenko beam), and (iii) a sandwich beam-column. The derivation holds for members in which the shortening due to the compressive load can be neglected. In all cases we choose the same approach, which is believed to appeal to structural engineers. The formula of the critical buckling load will increase in complexity for the successive cases in such a way that the next formula each time is a generalization of the preceding one. At the end we will confront the last derived formula with test results.

We consider a beam-column along the x-axis with deflection w in the z-direction due to a distributed loading p in z-direction. A thought experiment is done that we drill a tubelike hole of length l and small radius along the central axis of the beam, after which it is filled with a closely fitting chain of pin-connected rigid struts (see Fig. 6). It is assumed that no friction occurs between the strut chain and the face of the hole. The strut chain can be considered to be a cable, which is able to carry a compressive force, and therefore we will call it compressed cable hereafter. Compression forces P at the beam ends act on the compressed cable ($P > 0$). In the deflected state the structure behaves as a combination of beam and cable. The cable is of very large extensional rigidity and zero flexural and shear rigidities. For the time being one need not choose on whether an Euler–Bernoulli beam or a Timoshenko

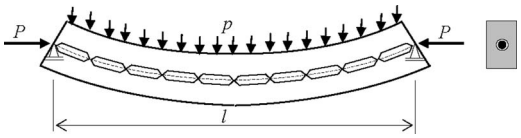

Fig. 6 A beam-column can be considered as a combination of a beam and a strut chain. Beam and strut chain are drawn in a deflected state.

beam is considered. The cable action can be studied independently of the choice about the beam theory. After the deformation of the beam the cable will be curved and a distributed downward line load q in the z-direction is acted by the compressed cable to the beam and reversely in opposite upward direction by the beam to the cable. In Fig. 7 an infinitesimal cable length dx is drawn in the deformed shape. Because the cable has no flexural and shear rigidities, the resultant force in the cable will be tangential to the cable axis in each cross section along the span. We decompose the cable force in a horizontal component and a vertical one. Because of equilibrium in x-direction, the horizontal component is P in each cross section. The transverse force in the cable depends on the slope of the beam axis and increases from left to right because of the increase in the slope of the beam axis in case of a positive second derivative of the deflection. The curved cable can only be in equilibrium if the upward distributed load q per unit length on the cable equals

$$q = -P\frac{d^2w}{dx^2} \tag{7}$$

Inspection of Fig. 7 reveals that the compressed cable analogy is in fact a translation of the Engesser hypothesis, where the shear force V is the product of the compressive force P and the inclination dw/dx of the center line of the member. It is stressed that the load $q = -P(d^2w/dx^2)$ applies regardless of which choice is made for the beam theory. Hence, it also applies for a beam-column of both finite flexural and shear rigidities and for sandwich columns.

4.1 Either Bending or Shear. We consider the limit case of flexural deformation only. The upward load q due to the beam on the cable is a downward load due to the cable on the beam-column. In the limit case of only bending the beam differential equation becomes

$$EI\frac{d^4w}{dx^4} = p + q \tag{8}$$

Accounting for Eq. (7) we obtain

$$EI\frac{d^4w}{dx^4} + P\frac{d^2w}{dx^2} = p \tag{9}$$

A solution of differential equation Eq. (9) for zero p, satisfying the support conditions $w = 0$ and $M = 0$, is $w(x) = \hat{w} \sin \alpha x$, where $\alpha = \pi/l$. Substitution in Eq. (9) transforms the relationship in $(\alpha^4 EI - \alpha^2 P)\hat{w} = 0$, from which the classical critical Euler buckling

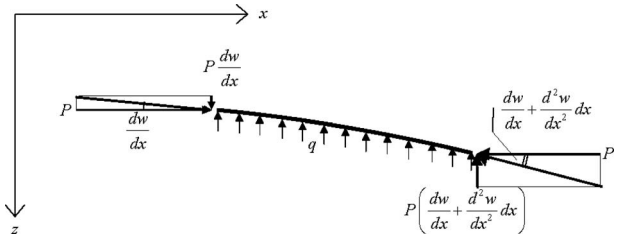

Fig. 7 Equilibrating forces on infinitesimal small compressed cable part; drawn at positive second derivative of the deflection *w*

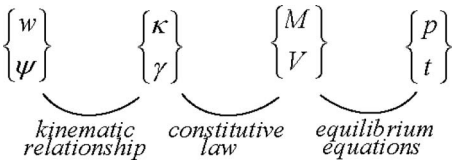

Fig. 8 Scheme of relevant quantities and their relationships in a member with both flexural and shear deformations

load $P_b=\alpha^2 EI$ is obtained.

In the case of only shear we obtain the differential equation

$$-GA_s\frac{d^2w}{dx^2}=p+q \tag{10}$$

which, accounting for Eq. (7), becomes

$$-GA_s\frac{d^2w}{dx^2}+P\frac{d^2w}{dx^2}=p \tag{11}$$

A solution of Eq. (11) is $w(x)=\hat{w}f(x)$, where $f(x)$ can be each deflection shape satisfying the support conditions $w=0$. Substitution in Eq. (11) transforms the relationship in $(-GA_s+P)\hat{w}=0$, from which the shear buckling load $P_s=GA_s$ is obtained.

4.2 Both Bending and Shear. Differential Eqs. (9) and (11) hold true for the limit cases of just flexural rigidity or just shear rigidity, respectively. Now differential equations are derived for the case in which the beam-column has both flexural and shear rigidities. We define two degrees of freedom w and ψ, which are the displacement of a cross section in the z-direction and the clockwise rotation of it, respectively. Two deformation quantities κ and γ occur for bending and shear, respectively. Two stress resultants correspond with these deformations, which are the bending moment M and the shear force V. Finally we distinguish external distributed loads p and t per unit length of the beam in the w- and ψ-directions, respectively. All these quantities are assembled in the scheme in Fig. 8. We will need kinematic relationships, constitutive laws, and equilibrium equations. The sign convention is shown in Fig. 9. The kinematic relationships are

$$\kappa=-\frac{d\psi}{dx};\quad \gamma=\frac{dw}{dx}-\psi \tag{12}$$

The constitutive laws are

$$M=EI\kappa;\quad V=GA_s\gamma \tag{13}$$

The equilibrium equations in w- and ψ-directions, respectively, are

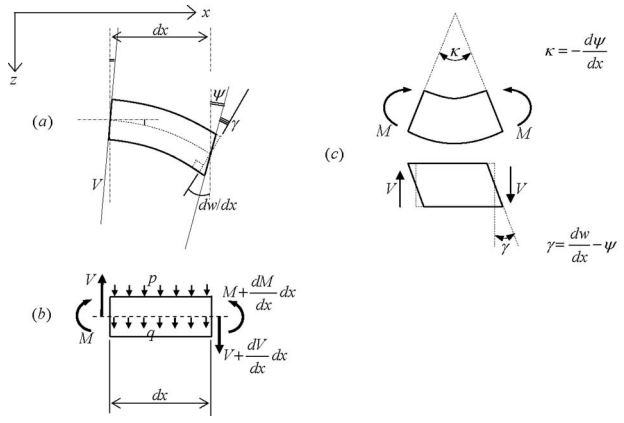

Fig. 9 Definition of curvature and shear strain; sign convention for moment and shear force

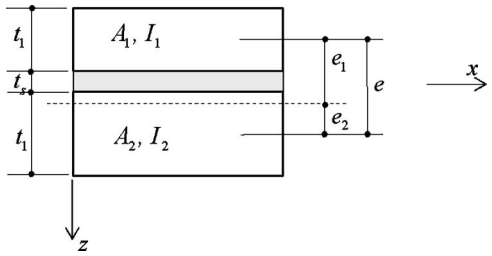

Fig. 10 Geometry of sandwich

$$-\frac{dV}{dx}=p+q;\quad \frac{dM}{dx}-V=t \tag{14}$$

Note that the load q due to the compressed cable is added in the equation for the equilibrium in w-direction, similar to Eqs. (8) and (10). The value of q is given in Eq. (7). By successive substitution of Eq. (12) into Eq. (13) and these new relationships in Eq. (14) transforms these equilibrium equations into

$$(P-GA_s)\frac{d^2w}{dx^2}+GA_s\frac{d\psi}{dx}=p$$

$$-GA_s\frac{dw}{dx}+\left(GA_s-EI\frac{d^2}{dx^2}\right)\psi=t \tag{15}$$

Substitution of the solution $w(x)=\hat{w}\sin\alpha x$ and $\psi(x)=\hat{\psi}\cos\alpha x$, which meets the member end conditions $M=0$ and $w=0$, and introducing corresponding loads $p(x)$ and $t(x)$, yields

$$\begin{bmatrix}\alpha^2(GA_s-P) & -\alpha GA_s\\ -\alpha GA_s & GA_s+\alpha^2EI\end{bmatrix}\begin{Bmatrix}\hat{w}\\ \hat{\psi}\end{Bmatrix}=\begin{Bmatrix}\hat{p}\\ \hat{t}\end{Bmatrix} \tag{16}$$

Note that a symmetric stiffness matrix is obtained. A nonzero solution for $\hat{w}$ and $\hat{\psi}$ for zero $\hat{p}$ and $\hat{t}$ requires solving the eigenvalue problem, setting the determinant of the stiffness matrix to zero. The condition for buckling becomes

$$GA_s\alpha^2EI-P(GA_s+\alpha^2EI)=0 \tag{17}$$

Accounting for Eq. (2), it can be rewritten as

$$PP_b+PP_s-P_bP_s=0 \tag{18}$$

which is similar to Eq. (3) in the derivation by Timoshenko and Gere. Solution (Eq. (5)) again applies, here alternatively written as

$$\frac{1}{P_{\rm cr}}=\frac{1}{P_b}+\frac{1}{P_s} \tag{19}$$

As could be expected, the classic result of Engesser is obtained.

4.3 Sandwich Column. Figure 10 shows the composition of a sandwich column and its position with respect to the x- and z-axis. We do not restrict the derivation to thin-faced sandwiches and start from a general thick-faced sandwich, which may be nonsymmetric. The face material is fully linear-elastic with modulus of elasticity E. The two layers are numbered 1 and 2, which numbers will be used as subscripts to quantities related to the face cross sections. The thicknesses are t_1 and t_2, the areas are A_1 and A_2, and the second-order moments are I_1 and I_2. The core material also is elastic and it is assumed that just shear stresses are considered; no normal stresses are taken into account. The shear modulus is G_s and the core thickness is t_s. The sandwich panel has a length l and width b and is simply-supported at both ends. The buckling load $P_{\rm cr}$ is applied in the neutral plane of the two faces, which occurs if they are ideally connected. This plane is on a distance e_1 to the center line of face 1 and distance e_2 to the center line of face 2. These distances are

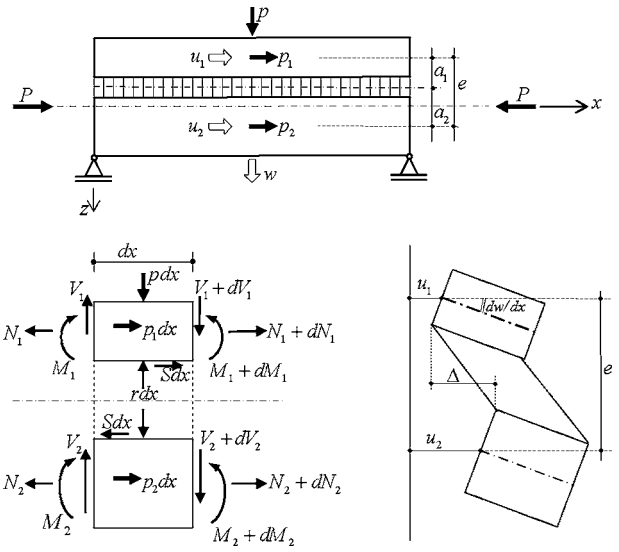

Fig. 11 Definition of the slip deformation and section forces in a sandwich; sign convention

$$e_1 = \frac{A_2}{A}e; \quad e_2 = \frac{A_1}{A}e \tag{20}$$

where

$$e = e_1 + e_2; \quad A = A_1 + A_2 \tag{21}$$

The sandwich is drawn again in Fig. 11. The displacements u_1, u_2, and w are independent degrees of freedom. Distributed loading can be applied in each of these three directions. We indeed introduce a distributed transverse load p per unit length of the sandwich in the w-direction and p_1 and p_2 in the directions of u_1 and u_2. The latter two do not occur in reality but are applied for the time being for reasons of completeness. In the course of the derivation we will put them to zero. The load p in the w-direction is applied on face 1, but will be partly transferred to face 2 by a distributed lateral force r in the core lateral to the faces. Here the compressed cable load q is applied to face 1, but this could be face 2 or a distribution over both without making any difference in the result.

Normal forces N_1 and N_2, bending moments M_1 and M_2, and shear forces V_1 and V_2 will occur in the faces. The strains ε_1 and ε_2 due to the normal forces and the curvature κ due to the bending moments (the same curvature in both faces) are taken into account, but the deformation due to the shear forces in the faces is neglected. A shear force S per unit length occurs in the midplane of the core. The deformation, which is associated with S, is a slip Δ of face 1 with respect to face 2. Because the deflection w is common to the two faces, it is convenient to sum up hereafter their flexural rigidity, bending moment, and shear force, introducing the total values EI_f, M_f, and V_f.

$$EI_f = EI_1 + EI_2; \quad M_f = M_1 + M_2; \quad V_f = V_1 + V_2 \tag{22}$$

The scheme in Fig. 12 summarizes the quantities which play a role in the laminated structural problem. It shows vectors for displacements, deformations, internal section forces, and external loading. The scheme is of great help in deriving the needed set of relations: (i) the kinematic relationships between displacements and deformations, (ii) the constitutive relationships between deformations and internal section forces, and (iii) the equilibrium relationships between the internal section forces and external loading. The bottom left-hand part of Fig. 11 shows which forces and moments act on differential sandwich parts of length dx. The picture shows the sign convention for all quantities. The bottom

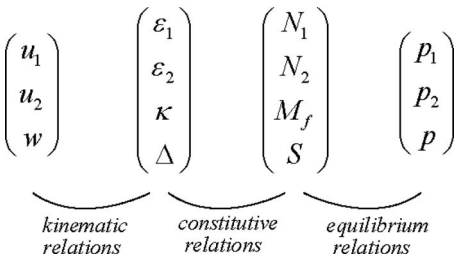

Fig. 12 Scheme of relevant quantities and their relationships in a sandwich member

right-hand part shows in which way the slip Δ is related to the displacements u_1, u_2, and dw/dx. The kinematic relationships are

$$\varepsilon_1 = \frac{du_1}{dx}; \quad \varepsilon_2 = \frac{du_2}{dx}; \quad \kappa = -\frac{d^2w}{dx^2}; \quad \Delta = -u_1 + u_2 + e\frac{dw}{dx} \tag{23}$$

The constitutive relationships are

$$N_1 = EA_1\varepsilon_1; \quad N_2 = EA_2\varepsilon_2; \quad M_f = EI_f\kappa; \quad S = k_s\Delta \tag{24}$$

Herein the core shear rigidity k_s is defined by

$$k_s = \frac{G_s b}{t_s} \tag{25}$$

The equations of equilibrium in the x-direction of the two faces can be directly written as

$$-\frac{dN_1}{dx} - S = p_1; \quad -\frac{dN_2}{dx} + S = p_2 \tag{26}$$

The relationship in the z-direction between the moment M_f, shear force S, and load p requires a number of intermediate steps. Equilibrium in the rotational direction of the two faces requires

$$\frac{dM_1}{dx} + a_1S - V_1 = 0; \quad \frac{dM_2}{dx} + a_2S - V_2 = 0 \tag{27}$$

Here a_1 is the distance between the center of the core and face 1, and similarly a_2 for face 2. They sum to e. Force equilibrium in the z-direction is satisfied by

$$p + q - r + \frac{dV_1}{dx} = 0; \quad r + \frac{dV_2}{dx} = 0 \tag{28}$$

Summing up the two relationships of Eq. (27) and similarly of Eq. (28), accounting for Eq. (22), yields

$$\frac{dM_f}{dx} + eS - V_f = 0; \quad p + q + \frac{dV_f}{dx} = 0 \tag{29}$$

The last step is to eliminate V_f from Eq. (29), with the result

$$-\frac{d^2M_f}{dx^2} - e\frac{dS}{dx} = p + q \tag{30}$$

This is the wanted equilibrium equation for the z-direction. Equations (23), (24), (26), and (30) are the basis for the derivation of the buckling formula. Substitution of Eq. (23) into Eq. (24) makes the section forces dependent on the displacements. Subsequently this result is substituted into the equilibrium equations (26) and (30), yielding three simultaneous differential equations when accounting for Eq. (7) as follows:

$$-EA_1\frac{d^2u_1}{dx^2} - k_s\left(-u_1 + u_2 + e\frac{dw}{dx}\right) = p_1$$

$$-EA_2\frac{d^2u_2}{dx^2} + k_s\left(-u_1 + u_2 + e\frac{dw}{dx}\right) = p_2$$

$$EI_f\frac{d^4w}{dx^4} - ek_s\left(-\frac{du_1}{dx} + \frac{du_2}{dx} + e\frac{d^2w}{dx^2}\right) + P\frac{d^2w}{dx^2} = p \tag{31}$$

Written in matrix form for zero distributed loading p_1, p_2, and p, we obtain the eigenvalue problem

$$\begin{bmatrix} -EA_1\frac{d^2}{dx^2} + k_s & -k_s & -ek_s\frac{d}{dx} \\ -k_s & -EA_2\frac{d^2}{dx^2} + k_s & ek_s\frac{d}{dx} \\ ek_s\frac{d}{dx} & -ek_s\frac{d}{dx} & EI_f\frac{d^4}{dx^4} + (P_{\mathrm{cr}} - e^2k_s)\frac{d^2}{dx^2} \end{bmatrix} \begin{bmatrix} u_1 \\ u_2 \\ w \end{bmatrix} = \begin{bmatrix} 0 \\ 0 \\ 0 \end{bmatrix} \tag{32}$$

The trial solution

$$u_1(x) = \hat{u}_1\cos\left(\frac{\pi x}{l}\right); \quad u_2(x) = \hat{u}_2\cos\left(\frac{\pi x}{l}\right); \quad w(x) = \hat{w}\sin\left(\frac{\pi x}{l}\right) \tag{33}$$

satisfies the boundary conditions, and transforms Eq. (32) into

$$\begin{bmatrix} k_1 + k_s & -k_s & -\frac{\pi}{l}ek_s \\ -k_s & k_2 + k_s & \frac{\pi}{l}ek_s \\ -\frac{\pi}{l}ek_s & \frac{\pi}{l}ek_s & \frac{\pi^2}{l^2}\{P_f + (e^2k_s - P_{\mathrm{cr}})\} \end{bmatrix} \begin{bmatrix} \hat{u}_1 \\ \hat{u}_2 \\ \hat{w} \end{bmatrix} = \begin{bmatrix} 0 \\ 0 \\ 0 \end{bmatrix} \tag{34}$$

where P_f and the stiffnesses k_1 and k_2 are defined as

$$P_f = \frac{\pi^2 EI_f}{l^2}; \quad k_1 = \frac{\pi^2 EA_1}{l^2}; \quad k_2 = \frac{\pi^2 EA_2}{l^2} \tag{35}$$

Again a symmetric stiffness matrix is obtained. Buckling occurs if nonzero displacements $\hat{u}_1$, $\hat{u}_2$, and $\hat{w}$ can occur for zero loading. This is the case when the determinant of the stiffness matrix in Eq. (34) becomes zero, which yields

$$(k_1k_2 + k_1k_s + k_2k_s)P_f + k_1k_2k_se^2 - (k_1k_2 + k_1k_s + k_2k_s)P_{\mathrm{cr}} = 0 \tag{36}$$

From this we solve the surprisingly simple buckling formula

$$P_{\mathrm{cr}} = P_f + \frac{e^2}{f_1 + f_s + f_2} \tag{37}$$

where the flexibilities in the denominator are

$$f_1 = k_1^{-1}; \quad f_s = k_s^{-1}; \quad f_2 = k_2^{-1} \tag{38}$$

In order to better interpret Eq. (37) we define two buckling loads P_o and P_s. Of these, P_o is the Euler buckling load of the sandwich member excluding the contribution P_f of the faces (in case of thin faces P_o is the real buckling load). It holds, accounting for Eqs. (20), (21), (35), and (38), that

$$P_o = \pi^2\frac{EI_o}{l^2} = \frac{e^2}{f_1 + f_2} \tag{39}$$

We define the buckling load P_s on basis of the core shear property

$$P_s = \frac{e^2}{f_s} \tag{40}$$

With reference to Eqs. (2), (25), and (38), we find

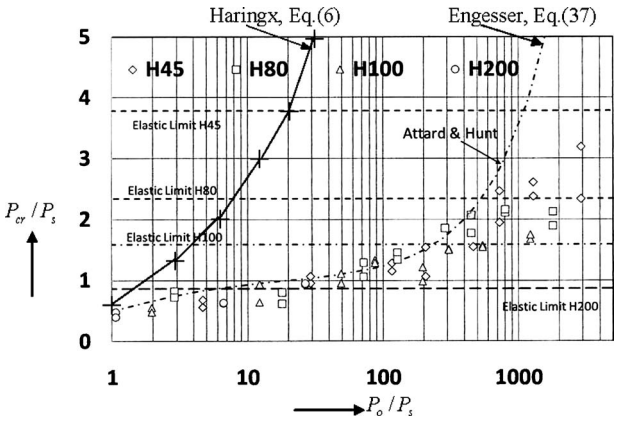

Fig. 13 Comparison of Eq. (37) (Engesser hypothesis) with test results of Attard and Hunt [18]

$$P_s = G_sA_s; \quad A_s = b\frac{e^2}{t_s} \tag{41}$$

Accounting for Eqs. (39) and (40), we can rewrite Eq. (37) as

$$P_{\mathrm{cr}} = P_f + \frac{1}{\frac{1}{P_o} + \frac{1}{P_s}} = P_f + \frac{P_oP_s}{P_o + P_s} \tag{42}$$

We easily recognize the Engesser formula in the right most part of the formula

$$P_{\mathrm{cr}} = P_f + P_{\mathrm{Engesser}}; \quad P_{\mathrm{Engesser}} = \frac{P_oP_s}{P_o + P_s} \tag{43}$$

If compared to the formula for P_{Engesser} in Eq. (5), the Euler buckling load P_b for only bending deformation is replaced by P_0. We conclude that the critical buckling load of any sandwich can be calculated by the Engesser solution P_{Engesser} for the sandwich considered as thin-walled, increased by the individual contribution P_f of the faces. The part P_{Engesser} cannot surpass the limit P_s, but this limit does not apply for the total critical buckling load P_{cr} because of the additional part P_f of the faces. It is stressed that the buckling mode is of macro-Euler type buckling; no typical shear buckling mode occurs.

Existing formulas by Sattler et al. [15] and Allen [16] appear after restructuring to be perfectly equivalent to the newly derived formula Eq. (42). Note that they all have been derived on the basis of the Engesser hypothesis.

4.4 Comparison of the Sandwich Buckling Formula to Test Results. For the comparison to test results we refer to the work of Attard and Hunt. In Ref. [13], they derived a formula for the prediction of the critical buckling load of sandwiches and have compared it with test results of Fleck and Sridhar [14] and Hoff and Mautner [17], proving that their formula is safe. At the same time they showed for thin-faced sandwiches that their prediction coincides perfectly with the existing prediction by the formula of Allen. In its turn the formula of Allen is the same formula as Eq. (37) and Eq. (42), both for thin-faced and thick-faced sandwiches. It remains surprising that the advanced hyperelastic formulation by Attard and Hunt and the present derivation (appealing to structural engineers) yield so close results.

In Ref. [18], Attard and Hunt published the results of tests they performed themselves. The figure in which they compare the experimental peak loads to their formula is copied here as Fig. 13. The symbols for the horizontal and vertical axes have been changed in accordance with the notation of the present paper. Because the tests regard thin-faced sandwiches we replaced $P_{\mathrm{euler}} = P_o + P_f$ on the horizontal axis by P_o. In the tests the dimensions of the sandwich were kept constant (face thickness of 1 mm,

core thickness of 10 mm), so the sandwich is of the thin-faced type. Therefore, the curve in this plot (the prediction by the formula of Attard and Hunt) is also the curve for Allen and Eq. (37). The latter two are based on the Euler hypothesis. Attard and Hunt applied four different core qualities (Divinicell H45, H80, H100, and H200 foams). As long as the sandwich members keep behaving elastic the correspondence between the test results and the prediction is good. When, in the tests, the elastic limit of the core material is approached, the results are much smaller than the predicted values. We conclude that Eq. (37) is in accordance with these test results and hence the Engesser hypothesis is adequate. Just for reasons of completeness we have added in the same plot the prediction by the Haringx formula of Eq. (6). It overestimates the buckling strength of the sandwich column in a very unsafe manner.

5 Conclusion

The formula of Haringx for critical buckling load has been proven to be correct for helical springs and elastomeric bearings. The present paper discusses the applicability of the Haringx theory for structural engineering purposes in building and civil engineering. For stability of structural members both the standard (Engesser) and the modified (Haringx) theories predict the correct limit value for shear-rigid members. This does not hold true for shear-weak members. Then the standard theory approaches a limit value for Timoshenko beam-columns, whereas the modified theory is derailing in an unsafe manner. It has not been sufficiently recognized that Haringx studied the lateral buckling of helical springs and remained in the shear-rigid domain in his theory and tests.

In the conventional application of the Engesser hypothesis the shear rigidity GA_s is the upper limit for the critical buckling load. However, the critical buckling load of shear-weak sandwich columns can surpass this limit by the critical buckling load of the individual faces when we choose the Engesser hypothesis. This buckling load of the individual faces can be of the same order of magnitude as the shear buckling load of a soft core sandwich column. It is negligible compared to the Euler buckling. The correspondence between the test results of Attard and Hunt and the prediction on the basis of the Engesser hypothesis justifies the use of the hypothesis. The expectation of Timoshenko and Gere that "the modified method (Haringx) may be more accurate for cases in which the effect of shear is unusually large" is not supported. We recommend to avoid the Haringx model in building and civil engineering and to choose for the Engesser hypothesis.

References

[1] Haringx, J. A., 1942, "On the Buckling and the Lateral Rigidity of Helical Compression Springs, I," Proc. K. Ned. Akad. Wet., **45**, pp. 533–539.

[2] Haringx, J. A., 1947, "On Highly Compressible Helical Springs and Rubber Bars and on Their Application in Vibration Isolation," Doctoral thesis, Delft University of Technology, The Netherlands.

[3] Grammel, R., 1924, "Die Knickung von Schraubenfedern," Z. Angew. Math. Mech., **4**, pp. 384–389.

[4] Biezeno, C. B., and Koch, J. J., 1925, "Zuschrift an den Herausgeber," Z. Angew. Math. Mech., **5**, pp. 279–280.

[5] Biezeno, C. B., and Grammel, R., 1953, *Technische Dynamik*, Springer-Verlag, Berlin.

[6] Engesser, F., 1891, "Die Knickfestigkeit gerader Stäbe," Zentrale Bauverwaltung, **11**, pp. 483–486.

[7] Ziegler, H., 1982, "Arguments for and Against Engesser's Buckling Formulas," Ing.-Arch., **52**, pp. 105–113.

[8] Timoshenko, S. P., and Gere, J. M., 1961, *Theory of Elastic Stability*, 2nd ed., McGraw-Hill, New York.

[9] Bažant, Z. P., 2003, "Shear Buckling of Sandwich, Fiber Composite and Lattice Columns, Bearings, and Helical Springs: Paradox Resolved," ASME J. Appl. Mech., **70**(1), pp. 75–83.

[10] Bažant, Z. P., and Beghini, A., 2004, "Sandwich Buckling Formulas and Applicability of Standard Computational Algorithm for Finite Strain," Composites, Part B, **35**, pp. 573–581.

[11] Bazant, Z. P., and Beghini, A., 2006, "Stability and Finite Strain of Homogenized Structures Soft in Shear: Sandwich or Fiber Composites, and Layered Bodies," Int. J. Solids Struct., **43**, pp. 1571–1593.

[12] Attard, M. M., and Hunt, G. W., 2008, "Column Buckling With Shear Deformations—A Hyperelastic Formulation," Int. J. Solids Struct., **45**, pp. 4322–4339.

[13] Attard, M. M., and Hunt, G. W., 2008, "Sandwich Column Buckling —A Hyperelastic Formulation," Int. J. Solids Struct., **45**, pp. 5540–5555.

[14] Fleck, N. A., and Sridhar, L., 2002, "End Compression of Sandwich Columns," Composites, Part A, **33**, pp. 353–359.

[15] Sattler, K., and Stein, P., 1974, *Ingenieurbauten 3, Theorie und Praxis*, Springer-Verlag, Wien.

[16] Allen, H. G., 1969, *Analysis and Design of Structural Sandwich Panels*, Pergamon, Oxford, UK, Chap. 8.

[17] Hoff, N. J., and Mautner, S. E., 1948, "Bending and Buckling of Sandwich Beams," J. Aeronaut. Sci., **15**, pp. 707–720.

[18] Attard, M. M., 2008, "Sandwich Column Buckling Experiments," *Futures in Mechanics of Structures and Materials*, Proceedings of the 20th Australasian Conference on the Mechanics of Structures and Materials, Toowoomba, University of Southern Queensland, Australia, pp. 373–377.